

PROPER MOTION OF THE LARGE MAGELLANIC CLOUD USING QSOs AS AN INERTIAL REFERENCE SYSTEM: THE Q0459–6427 FIELD

MARIO H. PEDREROS¹

Departamento de Física, Facultad de Ciencias, Universidad de Tarapacá, Casilla 7-D, Arica, Chile; mpedrero@uta.cl

AND

CLAUDIO ANGUITA^{1,2} AND JOSÉ MAZA¹

Departamento de Astronomía, Universidad de Chile, Casilla 36-D, Santiago, Chile; maza@das.uchile.cl

Received 2001 August 19; accepted 2002 January 7

ABSTRACT

The proper motion of the Large Magellanic Cloud relative to one background quasi-stellar object is determined using 44 CCD frames obtained from 1989.0 to 2000.0 at the Cassegrain focus of the Cerro Tololo Inter-American Observatory 1.5 m telescope. This is the continuation of a previous study made for three other LMC “quasar fields” observed with the same telescope and equipment and processed in a similar way. The results obtained here are compared with those by other authors who used different approaches and reference systems for the proper-motion determinations and with those in the previous study. The results of our proper-motion determination are in agreement with those of the former studies, but they show discrepancies when compared with the results of the latter. The possible causes of this inconsistency are discussed. Also, from the newly determined proper motion, the LMC spatial velocity vector is calculated, which in turn is used to determine the lower limit of the mass of the Galaxy contained within 50 kpc from its center.

Key words: astrometry — celestial mechanics — Magellanic Clouds — quasars: general

1. INTRODUCTION

One of the key parameters that has to be known for modeling the past history and evolution of the Magellanic Clouds (MCs) is their present spatial velocity vector. If this vector is known, it can be used as an initial condition in the calculations for the reconstruction and prediction of their past and future motion histories. Additionally, by assuming a reasonable value and distribution for the mass of the Galaxy, the velocity vector could help us decide whether or not the MCs are presently gravitationally bound to our Galaxy. One way to find the spatial velocity of the MCs is to observationally determine the proper motion of the two components, the Large and Small Magellanic Clouds (LMC and SMC, respectively).

Anguita, Loyola, & Pedreros (2000, hereafter ALP) determined the proper motion of the center of the LMC based on the study of three fields in it, each of which contains a background quasar (QSO), namely, Q0557–6713, Q0558–6707, and Q0615–6615. ALP used a method, hereafter referred to as the “quasar method,” consisting in taking the QSO as a fiducial point of reference to determine the proper motion of the LMC stars in the fields. As discussed below, their proper-motion determination yields results that differ from previous results obtained using methods relying on other reference systems. This is especially true in relation to their inferred value for and orientation of the LMC’s spatial velocity vector. This latter indicates that the LMC motion is nearly perpendicular to the motion predicted through theoretical models, such as those by Murai &

Fujimoto (1980), Lin & Lynden-Bell (1982), Shuter (1992), and Gardiner, Sawa, & Fujimoto (1994), and that its velocity is much too high for the LMC to be bound to the Galaxy, provided the current accepted value for the mass of the latter is assumed.

In this work we determine the LMC’s proper motion from the field containing the background QSO Q0459–6427. This is one of the “quasar fields” that was observed in conjunction with the fields in ALP and which had not been studied before. We compare the new results with those by ALP and other authors and discuss their consequences in relation to the nature of the LMC’s motion and the mass of the Galaxy.

2. OBSERVATIONS AND REDUCTIONS

The observational material was obtained (by C. A. and M. H. P.) with a CCD camera mounted on the Cerro Tololo Inter-American Observatory (CTIO) 1.5 m telescope at its Cassegrain $f/13.5$ focus and consists of 67 CCD frames of the LMC field around the quasar Q0459–6427 ($z = 2.0$, $V = 16.9$, $V-R = 0.32$) distributed in nine observation epochs ranging from 1989 through 2000. Most of the frames were taken through an R Johnson filter to reduce the effect of refraction; the rest were obtained through V and B Johnson filters in order to determine V , $B-V$, and $V-R$ magnitudes and colors for the field stars. Since the observations of this field were made at the same time as those for the three LMC fields in ALP, the type of CCD chips used, the observing epochs (up to 1996), and the fields of view and scales are the same as described in the latter reference. However, during the 1998–2000 epochs a TEK (1024 × 1024) chip with a scale of $0''.24 \text{ pixel}^{-1}$ and a $4'.1 \times 4'.1$ field of view was used (see Table 3). All chips used are thinned and back-side illuminated.

¹ Visiting Astronomer, Cerro Tololo Inter-American Observatory, National Optical Astronomy Observatory, which is operated by the Association of Universities for Research in Astronomy, Inc., under cooperative agreement with the National Science Foundation.

² Deceased.

As described by ALP, the quasar method consists in using the QSO in the field as a fiducial point to obtain the proper motion of the stars in it. This is done by assuming the QSO as the “moving target” and by selecting a set of stars in the LMC field as the reference stars with respect to which the “proper motion of the QSO” is measured. This selection has to meet certain photometric criteria fully explained in ALP. Since the reference stars belong to the LMC, they are what will actually move with respect to the QSO; thus the proper motion of the latter indeed corresponds to the “reflex” of the LMC field motion. We will therefore adopt the “negative” of the QSO motion as the proper motion of the mean center of the LMC reference stars in the studied field. Before calculating the proper motion, the (x, y) coordinates of the reference stars and quasar in each frame are corrected for differential color refraction and then transformed into “barycentric coordinates,” that is, coordinates referred to the mean reference star center of the corresponding frame. Since the coordinates of the quasar at different epochs must be referred to a common system of reference, a standard frame of reference (SFR) is defined by averaging the coordinates of the reference stars in three selected CCD frames taken in sequence on a good seeing night and with a good orientation of the chip relative to the celestial equatorial coordinate system. Then the newly calculated SFR coordinates for the reference stars are used, along with their observed barycentric counterparts, to identify the constant factors of the equations to transform the barycentric coordinates into the coordinates on the SFR system; this is done through multiple regression analysis by fitting both sets of data points to equations of the form: $X = a_0 + a_1 x + a_2 y + a_3 x^2$; $Y = b_0 + b_1 x + b_2 y + b_3 x^2$, where (X, Y) are the coordinates on the SFR system and (x, y) are the observed barycentric coordinates corrected for differential color refraction. The form of the equations above was adopted by testing equations of different forms to choose those that yielded the best fit to the data. Next, the newly found expressions are used to transform the (x, y) coordinates of the QSO (and also those for each reference star) for the different observing epochs onto the SFR (X, Y) coordinates. Once the coordinates on the SFR are calculated, the proper motion of the reference stars and QSO (apparent for the latter) are determined through an ordinary least-square regression analysis on X and Y versus epoch data points. Then a new selection of reference stars (kinematical in nature) is made by dropping from the sample all the stars with proper motions greater than 5 mas yr^{-1} , which are assumed not to belong to the LMC. Next an iterative process is carried out by recalculating the proper-motion components each time a new star is dropped, until the difference between old and new proper-motion values is less than or equal to 3σ . Once the final proper-motion values are secured, the “negative” of the apparent QSO’s proper motion is adopted as the proper motion of the mean LMC reference star center in the studied field.

Only 44 out of the 67 observed frames were actually used in the determination of the LMC proper motion. The rest were used in the determination of the differential color refraction correction coefficients, in obtaining the photometry for the stars and QSO, or simply were discarded for not meeting the requirements for inclusion in the proper-motion determinations. Table 1 shows the adopted parameters for the field centered on the quasar Q0459–6427. Figure 1 shows the 17 selected reference stars in the field, which are

TABLE 1
ADOPTED PARAMETERS FOR THE STUDIED LMC FIELD

Parameter	Q0459–6427 (deg)
R.A. (1950.0)	74.91
Decl. (1950.0).....	–64.45
l (1950.0), Galactic longitude.....	274.65
b (1950.0), Galactic latitude.....	–36.23
Position angle	–25.9
Θ , angular distance to LMC center.....	5.3

indicated by their identification number, and the QSO marked by two horizontal bars.

3. RESULTS

Figure 2 shows a V versus $B-V$ (a) and a V versus $V-R$ (b) color-magnitude diagrams of the stars in the studied field, reference stars are shown as open circles whereas the QSO is indicated as an upside down triangle. As seen from the figure, reference stars position themselves as actual LMC stars would do in this type of diagram. Table 2 lists the individual proper motions of each reference star along with their estimated uncertainties, corresponding to the error in the determination of the slope of the best-fit line. A map of the proper-motion data in Table 2 is presented in Figure 3, showing that the data is randomly scattered around the zero point. As Table 2 shows, the standard deviations of most reference stars are comparable to or larger than their proper-motion values, implying that we cannot assume that the proper-motion values quoted in Table 2 represent the actual relative motions of the stars in the LMC. This in turn means that the dispersion around the mean shown in Figure 3 and calculated to be ± 0.46 and $\pm 0.51 \text{ mas yr}^{-1}$ for the right ascension and declination components, respectively, probably stems entirely from the random errors in the measurements and does not represent the actual velocity dispersion in the LMC. Figure 4 shows the position versus epoch diagrams for the QSO in right ascension (Fig. 4a) and declination (Fig. 4b), relative to the (moving) standard reference frame. Symbol sizes and shapes in this diagram are related to the number of times the measurements yielded the same coordinate value for a particular epoch. The best-fit straight lines resulting from linear regression analyses on the data points are also shown. As explained above, the negative values of the best-fit line slopes correspond to the proper motion of the mean center of the reference stars in the studied field, and their values are $\mu_\alpha \cos(\delta) = (+1.8 \pm 0.2) \text{ mas yr}^{-1}$ and $\mu_\delta = (+0.3 \pm 0.2) \text{ mas yr}^{-1}$ for right ascension and declination, respectively, measured over a total of 44 CCD frames distributed in nine epochs of observation. Table 3 lists the CCD chips used throughout this program along with the mean barycentric positions of the QSO, their mean errors, and the number of points used to calculate the mean for each coordinate and epoch. Note that the rather small quoted errors for the proper motion come out directly from what the least-square fit program yields as the uncertainty in the determination of the slope of the best-fit line. At this point it is important to emphasize the fact that several authors (e.g., Monet 1992; Harris et al. 1998) state that on a good night a good star can be measured to astrometric accuracies of 3 mas. This figure

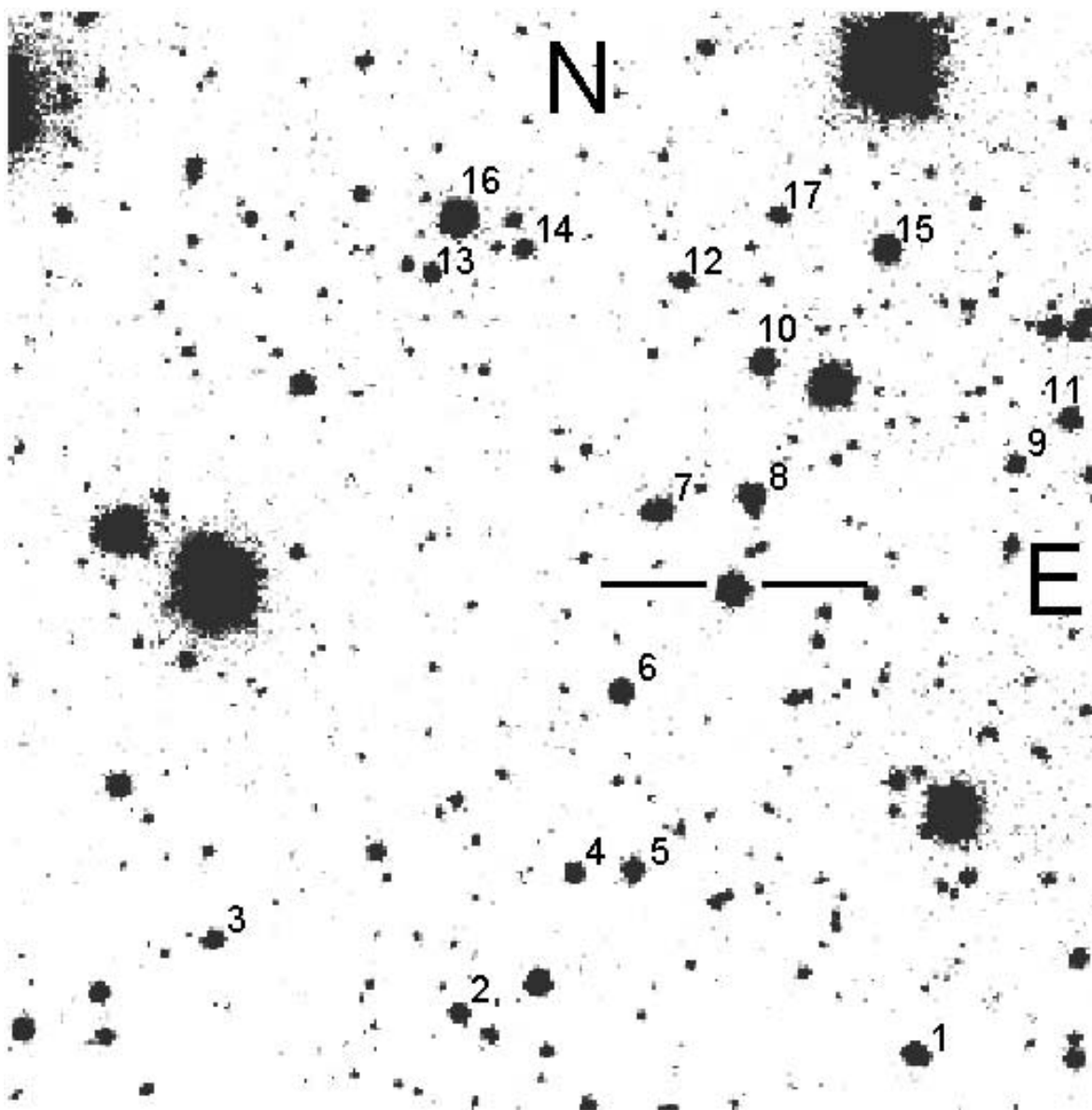


FIG. 1.—Finding charts of the reference stars and QSO (indicated by the two bars) for the field Q0459–6427. The chart covers a $2' \times 2'$ field

was confirmed by C. Anguita (1999, private communication) who obtained similar results from 36 SMC stars in six frames observed with the same equipment used in this work. Therefore, if we assume an accuracy of 3 mas for a single observation, we can make a rough estimation of the kind of errors we should be obtaining in our proper-motion measurement. As we have an average of five observations per epoch per field, the mean error per epoch should amount to $3/5^{1/2} = 1.3$ mas. On a time basis of 10 yr this translates into an uncertainty on the proper-motion measurement of $(1.3^2 + 1.3^2)^{1/2} / 10 = 0.18$ mas yr⁻¹. The latter value is in total agreement with the uncertainties quoted above for our proper-motion determination. Besides, it should be noted that the above calculations are based only on an initial and final epochs, separated by 10 years, whereas in our case we are dealing with a total of nine observing epochs, which makes our results much more reliable because of the larger amount of information being used in the calculations.

It is also interesting to note that in this method the proper motion is not referred to any particular celestial coordinate system but is tied directly to the quasar without any intermediary. This makes the results totally independent from any particular absolute system of reference (and its associated errors).

4. COMPARISON WITH PREVIOUS MEASUREMENTS

Table 4 lists the results of all measurements, with uncertainties of less than 1 mas yr⁻¹ in both μ components, that are known for the LMC's proper motion and the system of reference used for the measurements. Proper-motion values from Jones, Klemola, & Lin (1994), ALP, and this work are given for the center of rotation of the LMC. These values are obtained by correcting the field proper motion for rotation of the LMC plane and for solar motion. The total LMC proper

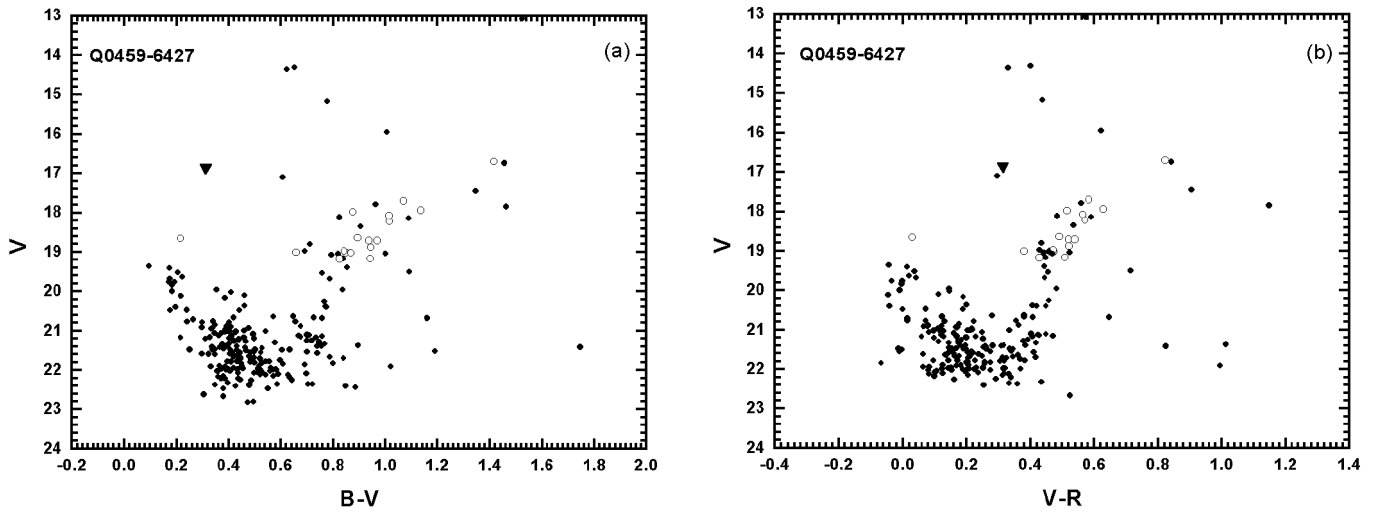


FIG. 2.— V vs. $B-V$ (a) and V vs. $V-R$ (b) color-magnitude diagrams for stars within the $2' \times 2'$ field surrounding the QSO Q0459–6427. The diagram shows a typical LMC stellar population with almost no contamination. The stars chosen to define the standard frame of reference are shown as open circles, whereas the QSO is indicated by an upside down triangle.

motion obtained here amounts to $\mu = (+2.0 \pm 0.2)$ mas yr^{-1} with a position angle $\theta = 79^\circ$ measured eastward from the meridian joining the center of the LMC to the north pole. This value is compatible with theoretical models mentioned in § 1, which predict a proper motion of the LMC in the range 1.5–2.0 mas yr^{-1} with a position angle $\theta \approx 90^\circ$. As for the SMC, Gardiner et al. (1994) predict a proper motion of $\mu = +1.6$ mas yr^{-1} with $\theta = 50^\circ$. Strangely enough, although our values are in agreement with most of the observational measurements shown in Table 4, they show a significant discrepancy with those from ALP, for which the observations were done at the same time and with the same equipment as

those in this work. We will come back to this last point in the next section.

5. SPATIAL VELOCITY OF THE LMC AND MASS OF THE GALAXY

In this section we calculate the radial and tangential components of the velocity of the LMC’s center as seen from the center of the Galaxy, following the steps prescribed by Jones et al. (1994). For this we use the proper-motion determination in § 3 and adopt a value for the radial velocity of the LMC’s center. The LMC parameters adopted for this calculation are those in ALP (see their Table 8). Before using the

TABLE 2
STELLAR REFERENCE FRAME FOR THE Q0459–6427 FIELD

Star	$\mu_\alpha \cos \delta$ (mas yr^{-1})	σ (mas yr^{-1})	μ_δ (mas yr^{-1})	σ (mas yr^{-1})	V	$B-V$	$V-R$
1.....	−0.2	0.4	+1.0	0.2	18.71	0.95	0.52
2.....	−1.0	0.3	+0.2	0.4	19.01	0.67	0.38
3.....	+0.6	0.2	−0.7	0.2	19.02	0.86	0.47
4.....	+0.1	0.3	−0.3	0.3	18.88	0.96	0.52
5.....	+0.1	0.3	+0.6	0.3	18.71	0.98	0.54
6.....	+0.0	0.2	−0.4	0.2	18.22	1.03	0.58
7.....	+0.3	0.5	−0.3	0.5	18.08	1.03	0.57
8.....	+0.3	0.2	+0.2	0.2	17.98	0.89	0.52
9.....	−0.1	0.3	−0.7	0.4	19.18	0.84	0.43
10.....	+0.3	0.1	0.0	0.3	17.94	1.15	0.63
11.....	0.0	0.3	+0.4	0.3	18.64	0.91	0.50
12.....	+0.2	0.3	−1.1	0.3	19.03	0.88	0.48
13.....	+0.3	0.3	+0.6	0.3	18.98	0.86	0.48
14.....	−0.9	0.3	0.0	0.3	18.66	0.23	0.03
15.....	−0.1	0.1	−0.1	0.2	17.70	1.08	0.59
16.....	+0.2	0.2	+0.6	0.2	16.70	1.43	0.82
17.....	−0.2	0.3	+0.4	0.3	19.17	0.95	0.51

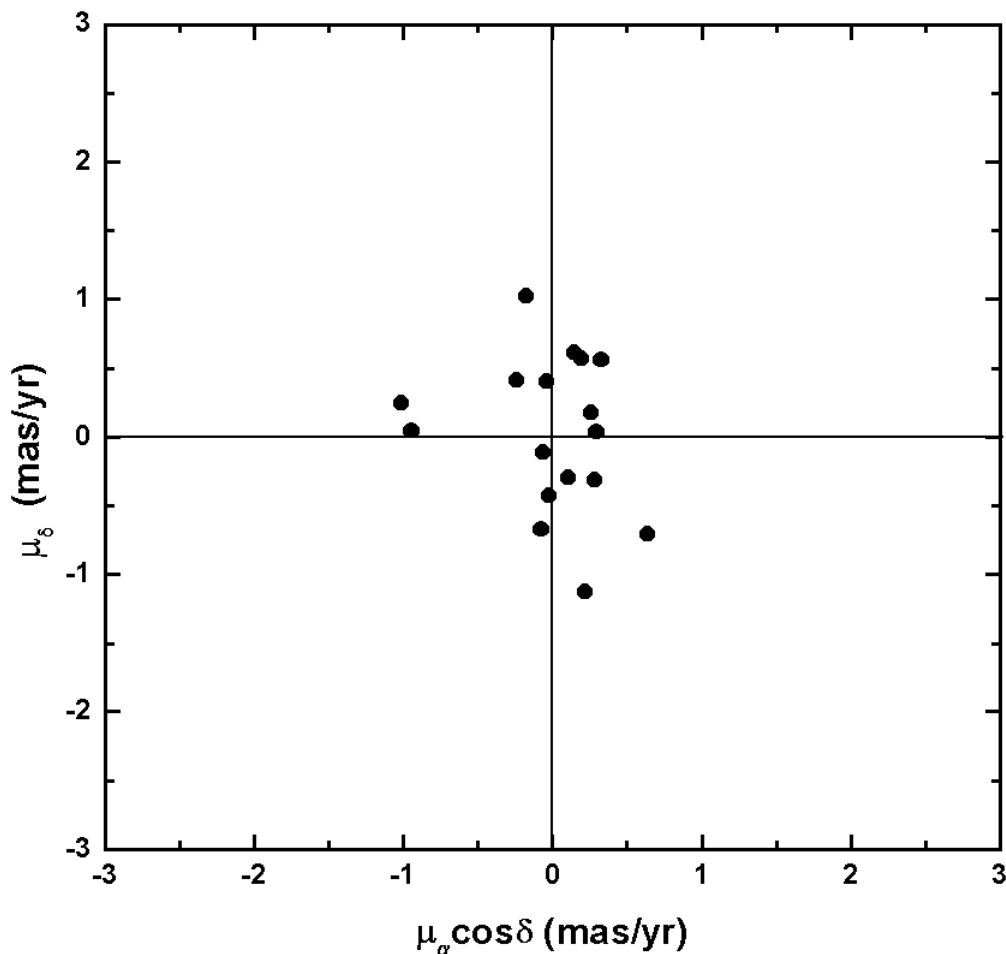


FIG. 3.—Proper-motion map for the 17 reference stars in the studied LMC field that are listed in Table 2

measured proper motions to derive the spatial velocity vector, it is necessary to follow a series of steps (explained in more detail in ALP). The first step deals with the proper-motion correction arising from the rotation of the LMC's

plane; here we have to express the rotational velocity v_Φ in terms of its components ($v_{\Phi\alpha}$, $v_{\Phi\delta}$, $v_{\Phi r}$) on the equatorial coordinate system centered on the field. Assuming a rotational velocity $v_\Phi = 50 \text{ km s}^{-1}$ and a radial velocity

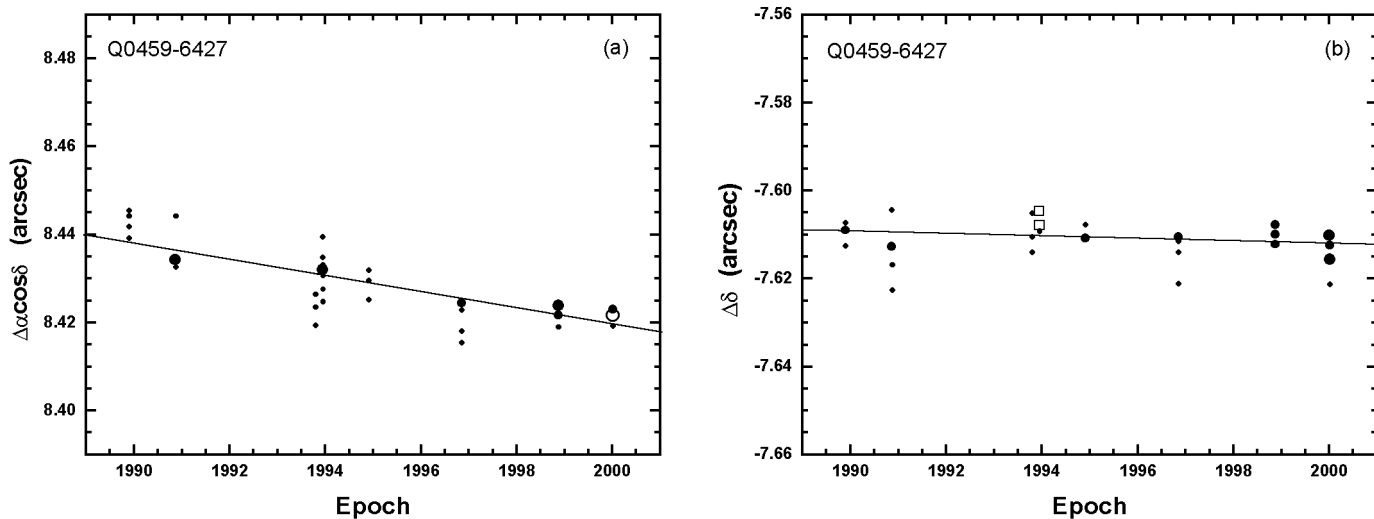


FIG. 4.—Right ascension ($\Delta\alpha \cos \delta$) and declination ($\Delta\delta$) vs. epoch of observation for Q0459–6427. The values of $\Delta\alpha \cos \delta$ and $\Delta\delta$ represent the positions of the QSO on different CCD frames relative to the barycenter of the standard frame of reference. The point sizes are proportional to the number of times the measurement yielded the same coordinate value for a particular epoch (*small, medium, and large*: one, two, and three measurements epoch⁻¹, respectively; *open square and circle*: four and six measurements epoch⁻¹, respectively). The best-fit straight line from linear regression analyses on the data points is also shown.

TABLE 3
MEAN BARYCENTRIC POSITIONS OF THE QUASAR Q0459–6427

Epoch	$\Delta\alpha \cos(\delta)$ (arcsec)	σ (mas)	N	$\Delta\delta$ (arcsec)	σ (mas)	N	CCD Chip
1989.907.....	8.443	1.4	4	-7.609	1.1	4	RCA No. 5
1990.872.....	8.434	0.3	3	-7.610	2.8	3	Tek No. 4
1990.878.....	8.438	5.8	2	-7.620	2.8	2	RCA No. 5
1993.800.....	8.423	2.0	3	-7.610	2.6	3	Tek 1024 No. 1
1993.953.....	8.432	1.4	9	-7.607	0.6	9	Tek 1024 No. 2
1994.916.....	8.429	2.0	3	-7.610	1.0	3	Tek 1024 No. 2
1996.860.....	8.421	1.8	5	-7.614	2.0	5	Tek 2048 No. 4
1998.881.....	8.422	0.8	6	-7.610	0.8	6	Tek 1024 No. 2
2000.010.....	8.422	0.4	9	-7.614	1.2	9	Tek 1024 No. 2

TABLE 4
HIGH-PRECISION DETERMINATIONS OF THE LMC PROPER MOTION

Source	$\mu_\alpha \cos(\delta)$ (mas yr ⁻¹)	μ_δ (mas yr ⁻¹)	Proper-Motion System
Kroupa, Röser, & Bastian 1994 (field).....	+1.3 ± 0.6	+1.1 ± 0.7	PPM
Jones et al. 1994 (LMC center).....	+1.37 ± 0.28	-0.18 ± 0.27	Galaxies
Kroupa & Bastian 1997 (field).....	+1.94 ± 0.29	-0.14 ± 0.36	Hipparcos
Anguita et al. 2000 (LMC center).....	+1.7 ± 0.2	+2.9 ± 0.2	Quasars
This work (LMC center).....	+2.0 ± 0.2	+0.4 ± 0.2	Quasars

$V_r = 250 \text{ km s}^{-1}$, we obtain $(-40, -21, 21) \text{ km s}^{-1}$ for the above components. In the second step the $v_{\Phi\alpha}$ and $v_{\Phi\delta}$ components are transformed into $\Delta\mu_\alpha$ and $\Delta\mu_\delta$, that is, the corrections to be applied to $\mu_\alpha \cos(\delta)$ and μ_δ to account for the rotation of the LMC's plane. The third step corresponds to the calculation of the corrected proper-motion values and their transformation into the velocity components, V_α and V_δ in the local equatorial system centered on the field. In the fourth step, through a rotation around the line of sight, we transform the previous components into V_l and V_b , i.e., their equivalent in the Galactic coordinate system centered on the field. The fifth step consists in transforming the latter two components, along with the radial velocity of the LMC's center, into a coordinate system centered on the Sun, from which the velocity components of the solar motion are subtracted to obtain $(V_{hc,l}, V_{hc,b}, V_{hc,r})$, i.e., the

Galactic longitude, latitude, and radial velocity components of the motion of the LMC's center in the coordinate system centered on the motionless Sun. The sixth and last step consists in transforming the above components into the transverse ($V_{gc,t}$) and radial ($V_{gc,r}$) velocity of the LMC's center, as seen from the Galactic center. The numerical results from these calculations are listed in Table 5.

If we assume that the LMC is gravitationally bound to and in an elliptical orbit around the Galaxy, and that the mass of the Galaxy is contained within 50 kpc of the galactic center, we can make an estimate of the lower limit of this mass through the expression:

$$M_G = (r_{\text{LMC}}/2G)[V_{gc,r} + V_{gc,t}(1 - r_{\text{LMC}}^2/r_a^2)] / (1 - r_{\text{LMC}}/r_a),$$

where r_a is the LMC's apogalacticon distance, and r_{LMC} the LMC's present distance. For $r_a = 300 \text{ kpc}$ (Galaxy's tidal radius) we obtain

$$M_G = (8.8 \pm 1.5) \times 10^{11} M_\odot.$$

TABLE 5
VELOCITY RESULTS FOR THE LMC

Parameter	Q0459–6427
η , angle of the star.....	257°9
$\Delta\mu_\alpha \cos \delta$, R.A. proper-motion correction (mas yr ⁻¹).....	-0.17
$\Delta\mu_\delta$, Decl. proper-motion correction (mas yr ⁻¹).....	-0.09
V_α , field R.A. velocity (km s ⁻¹).....	478 ± 46
V_δ , field decl. velocity (km s ⁻¹).....	88 ± 46
V_r , field radial velocity (km s ⁻¹).....	243 ± 10 ^a
$V_{hc,l}$, LMC heliocentric velocity (km s ⁻¹).....	-140 ± 45
$V_{hc,b}$, LMC heliocentric velocity (km s ⁻¹).....	-244 ± 22
$V_{hc,r}$, LMC heliocentric velocity (km s ⁻¹).....	225 ± 30
$V_{gc,r}$, LMC Galactocentric velocity (km s ⁻¹).....	82 ± 25
$V_{gc,t}$, LMC Galactocentric velocity (km s ⁻¹).....	350 ± 31

^a Values adopted to make the radial velocity of the LMC's center equal to $250 \pm 10 \text{ km s}^{-1}$.

TABLE 6
MASS OF THE GALAXY FOR TWO LMC ROTATIONAL VELOCITIES

Parameter	Q0459–6427
For $v_\Phi = 0 \text{ km s}^{-1}$:	
$V_{gc,r}$, LMC Galactocentric velocity (km s ⁻¹).....	78 ± 25
$V_{gc,t}$, LMC Galactocentric velocity (km s ⁻¹).....	306 ± 30
M_G , mass of the Galaxy (M_\odot).....	$(6.8 \pm 1.3) \times 10^{11}$
For $v_\Phi = 90 \text{ km s}^{-1}$:	
$V_{gc,r}$, LMC Galactocentric velocity (km s ⁻¹).....	86 ± 25
$V_{gc,t}$, LMC Galactocentric velocity (km s ⁻¹).....	385 ± 31
M_G , mass of the Galaxy (M_\odot).....	$(11.0 \pm 1.7) \times 10^{11}$

Calculations similar to those above were carried out assuming $v_{\Phi} = 0 \text{ km s}^{-1}$ (zero rotation) and $v_{\Phi} = 90 \text{ km s}^{-1}$ for the LMC's rotational velocity. The results of these new calculations are given in Table 6 for the galactocentric radial and transverse velocity of the LMC and for the corresponding mass of the Galaxy as defined above. All the above results indicate that the assumption that the LMC is bound to the Galaxy results in a mass value for the Galaxy which is compatible with the theoretical $7 \times 10^{11} M_{\odot}$ value, the upper mass limit estimated from the models mentioned in § 1.

In the following paragraph we give some thought to trying to understand the discrepancy between the results obtained in this work and those by ALP.

First, the fact that the observations used here were made at the same time and with the same equipment as those by ALP precludes any arguments relating the discrepancy to the presence of systematic errors in the observational data, since these would affect our data in the same way as those of ALP. Second, concerning the processing of the data, we used the same procedure as ALP (through DAOPHOT/IRAF) to obtain the centroid coordinates (x, y) for each reference star and the QSO. The subsequent procedures to obtain the proper motion were also basically the same, except that in our case we wrote special software routines to make the processing semiautomatic and included a quadratic term in the transformation equations that is not included in ALP's equations. We are planning to reprocess ALP's data through our software to see if any differences show up. In any case, we suspect that including this quadratic term in the reprocessing of ALP's data will only marginally affect their proper-motion values in right ascen-

sion and will do nothing to the proper-motion value in declination, which is the conflicting component. A third argument is that these discrepancies might be related to the fact that the field studied here is located at a different right ascension and distance from the LMC's center and in a position diametrically opposed to the fields studied by ALP; any peculiarities in the rotation curve of the LMC's plane between both positions would not be accounted for by the rotation correction applied here. Last, the presence of any peculiar motions within the LMC, such as "streaming," for example, would distort the proper-motion determinations that were made assuming no peculiarities in the motion of the stars in both our and ALP's fields. It would then be important to try to check the last two arguments if no positive explanation is obtained from the second point above.

We conclude that, since our results are compatible with those by other authors both theoretically and observationally, it becomes necessary to reanalyze ALP's results in order to understand the reason why their proper-motion values (particularly in declination) differ so significantly from those found in this work, in spite of having used the same method of analysis, the same observational equipment, and having done the observations in the same epochs.

This work was partly financed through the Universidad de Tarapaca research fund (project No. 4721-99). We are grateful to W. van Altena and T. Girard for reading the manuscript and for helpful comments and suggestions. We are indebted to an anonymous referee for helping to make this a better work. We also thank E. Navea for helping us with the processing of the data and figures.

REFERENCES

- Anguita, C., Loyoya, P., & Pedreros, M. H. 2000, *AJ*, 120, 845 (ALP)
 Gardiner, L. T., Sawa, T., & Fujimoto, M. 1994, *MNRAS*, 266, 567
 Harris, H. C., et al. 1998, *ApJ*, 502, 437
 Jones, B. F., Klemola, A. R., & Lin, D. N. G. 1994, *AJ*, 107, 1333
 Kroupa, P., & Bastian, U. 1997, *NewA*, 2, 77
 Kroupa, P., Röser, S., & Bastian, U. 1994, *MNRAS*, 266, 412
 Lin, D. N. C., & Lynden-Bell, D. 1982, *MNRAS*, 198, 707
 Monet, D. G. 1992, in *ASP Conf. Ser. 23, Astronomical CCD Observing and Reduction Techniques*, ed. Steve B. Howell (San Francisco: ASP)
 Murai, T., & Fujimoto, M. 1980, *PASJ*, 32, 581
 Shuter, W. L. 1992, *ApJ*, 386, 101